

This thesis is dedicated

to

my beloved

parents & family



Statement by author

This dissertation fulfills the partial requirements for the award of an advanced degree at the University of North Bengal (NBU) and is archived in the university library for lending following NBU regulations. Limited excerpts from this dissertation may be utilized without specific permission as long as proper acknowledgment of the source is provided. Requests for extensive reproduction or quoting from this manuscript, whether in whole or in part, can be considered by authorized personnel at NBU if deemed beneficial for academic purposes. Alternatively, permission must be obtained directly from the author.

Arpita Maiti

Declaration

I hereby assert that the thesis titled "**Probing Assorted Host-Guest Interactions Prevailing in Various Environments to Explore Different Target Analytes by Diverse Spectroscopic Contrivances**" represents the culmination of my original research. This work was conducted under the guidance of Prof. (Dr.) M N Roy (Supervisor) and Dr. Tanusree Ray (Co-supervisor) at the Department of Chemistry, University of North Bengal.

The content of this thesis is the outcome of my independent investigation, showcasing my dedicated efforts and comprehension of the subject matter. The data, results, and conclusions presented in this document are derived from authentic research findings and have not been previously submitted for any other degree or qualification, either at this institution or elsewhere.

I affirm that the content of this thesis is a genuine reflection of my research work, presented with the utmost honesty and integrity.

Arpita Maiti
.....

Arpita Maiti

Department of Chemistry

University of North Bengal

Darjeeling-734013

West Bengal, India

Date:

UNIVERSITY OF NORTH BENGAL

PROF (DR.) M. N. ROY

FRSC (London), UK

Senior Professor of Chemistry, NBU

Founder Vice-Chancellor of

Alipurduar University

Awardee of One Time Grant from UGC,

Prof. Suresh C. Ameta Award from ICS,

Bronze Medal from CRSI

and

Shiksha Ratna, Dooars Ratna and Banga

Bhushan from the Government of West

Bengal



‘समानो मन्त्र समिति समानी’

Phone: 0353 2776381

Mobile: 094344 96154

Fax: +91 353 2699001

Darjeeling-734 013,

West Bengal, INDIA

April, 2024

Email: mahendraroy2002@yahoo.co.in
/mahendraroy2018@nbu.ac.in

CERTIFICATE

I certify that Mrs. Arpita Maiti has prepared the thesis entitled “**Probing Assorted Host-Guest Interactions Prevailing in Various Environments to Explore Different Target Analytes by Diverse Spectroscopic Contrivances**” for the award of the Ph.D. degree of the University of North Bengal, under our guidance. She has carried out research work at the Department of Chemistry, University of North Bengal.

Mahendra Nath Roy

Prof. (Dr.) Mahendra Nath Roy

(Supervisor)

Professor of Chemistry

Department of Chemistry

University of North Bengal

Darjeeling – 734013

West Bengal, India

Date: *08-04-2024.*

Prof. (Dr.) M. N. Roy
FRSC (London), UK
Department of Chemistry
University of North Bengal
Darjeeling-734013, India



**DEPARTMENT OF CHEMISTRY
SILIGURI COLLEGE**

(Govt. Sponsored)
NAAC Accredited Grade B++
P.O. Siliguri : Dt. Darjeeling, Pin - 734001

CERTIFICATE

I certify that Mrs. Arpita Maiti has prepared the thesis entitled **“Probing Assorted Host-Guest Interactions Prevailing in Various Environments to Explore Different Target Analytes by Diverse Spectroscopic Contrivances.”** for the award of **Ph.D. (Doctor of Philosophy)** degree of the University of North Bengal, under our guidance. She has carried out research work at the Department of Chemistry, University of North Bengal.

Tanusree Ray

Dr. Tanusree Ray

(Co-supervisor)

Assistant Professor

Department of Chemistry

Siliguri College

Siliguri, 734001

West Bengal, India

Dated: *08.04.2024*

Dr. Tanusree Ray
Asstt. Professor In Chemistry
Siliguri College

Anti-plagiarism report



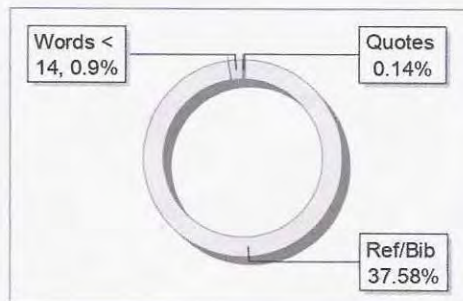
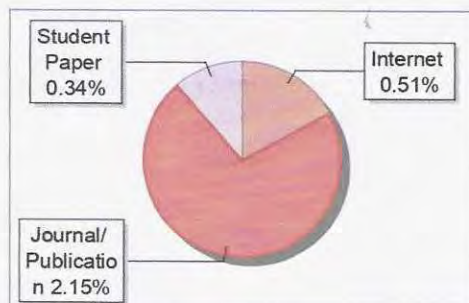
The Report is Generated by DrillBit Plagiarism Detection Software

Submission Information

Author Name	Arpita Maiti
Title	Probing Assorted Host-Guest Interactions Prevailing in Various Environments to Explore Different Target Analytes by Diverse Spectroscopic Contrivances
Paper/Submission ID	1590089
Submitted by	nbuplg@nbu.ac.in
Submission Date	2024-04-01 11:05:13
Total Pages	152
Document type	Thesis

Result Information

Similarity **3 %**



Exclude Information

Quotes	Excluded
References/Bibliography	Excluded
Sources: Less than 14 Words %	Not Excluded
Excluded Source	1 %
Excluded Phrases	Not Excluded

Database Selection

Language	English
Student Papers	Yes
Journals & publishers	Yes
Internet or Web	Yes
Institution Repository	Yes

A Unique QR Code use to View/Download/Share Pdf File



Melinda Naik Roy
(08-04-2024)

Tanusree Ray
(08.04.2024)

Prof. (Dr.) M. N. Roy
FRSC (London), UK
Department of Chemistry
University of North Bengal
Darjeeling-734013, India

Dr. Tanusree Ray
Asstt. Professor In Chemistry
Siliguri College

Arpita Maiti
08.04.2024

Preface

With immense joy and a profound sense of achievement, I am delighted to present my doctoral thesis, titled "**Probing Assorted Host-Guest Interactions Prevailing in Various Environments to Explore Different Target Analytes by Diverse Spectroscopic Contrivances.**" This thesis marks the culmination of my journey toward attaining a Doctor of Philosophy (Ph.D.) degree in Chemistry, showcasing the dedicated efforts and unwavering passion that have propelled me throughout my academic pursuit. My enrollment in the Ph.D. program at the University of North Bengal commenced on January 2, 2019, as indicated by letter no. Ph.D./Chem. (1922)/248/R-2024, under the esteemed guidance of Prof. (Dr.) M. N. Roy and Dr. Tanusree Ray, Siliguri College. This scholarly venture was initiated to delve into the intriguing realm of probing assorted host-guest interactions prevailing in various environments to explore different target analytes by diverse spectroscopic contrivances

The motivation driving this research emanated from the burgeoning interest in comprehending probing assorted host-guest interactions prevailing in various environments to explore different target analytes by diverse spectroscopic contrivances. These host-guest interactions prevailing in various environments to explore different target analytes exhibit captivating properties with potential applications in food technology, environmental research, environmental security programs. Unraveling the underlying mechanisms governing host-guest interactions to explore different target analytes and exploring their practical applications has been the driving force behind the present investigation.

I express my profound gratitude to my esteemed supervisor, Prof. (Dr.) M. N. Roy, and co-supervisor, Dr. Tanusree Ray, Siliguri College, whose extensive knowledge, expertise, and guidance have played a pivotal role in shaping the direction of this research. Their constant encouragement, invaluable insights, and constructive feedback have served as guiding beacons, illuminating my path during moments of uncertainty.

Additionally, I extend my heartfelt thanks to the Department of Chemistry at the University of North Bengal for fostering a nurturing academic environment and providing access to state-of-the-art facilities, which proved indispensable in conducting the present thesis research work.

Acknowledgments

I express my sincere gratitude to **Prof. (Dr.) M. N. Roy**, my Ph.D. supervisor, and **Dr. Tanusree Ray**, my Ph.D. co-supervisor, Siliguri College for their invaluable scientific assistance and unwavering support during my research. Their extensive knowledge and passion for science have consistently inspired me, driving me to excel in the laboratory. Working with them has been a privilege, and I appreciate their patience in meticulously reviewing this thesis.

I extend my heartfelt thanks to the members of my thesis committee for their valuable suggestions and guidance throughout my research journey. I also acknowledge the support of Prof. (Dr.) B. Biswas, the Head of the Department of Chemistry at the University of North Bengal. I am also grateful to Prof. (Dr.) Pranab Ghosh and Prof. (Dr.) B. Sinha former Head of the Department of Chemistry at the University of North Bengal. My gratitude extends to all faculty members in the Department of Chemistry for their support, encouragement, and role modeling that has shaped my academic career.

Special appreciation goes to my lab members and all co-authors in my publications especially Manas Mahato, Sabbir Ahamed, Najmin Tohora, and Tuhina Sultana whose collaboration has been a delightful experience. I am equally thankful to all my teachers throughout my life especially, my uncle Prankrishna Maiti, Subhas Kumar Maity, Bulu and Bankim Adhikary, Alok Samanta, Elora Banerjee, Sumana Bhadra, Late Samar Chakraborty, Late Samarendra Nath Das, Late Debendranath Misra, Sisir Maity, Dr. Sudhir Pal, Dr. Nirmal Kumar Hazra, Dr. Anup Dasmahapatra, Dr. Mahadev Maity, Dr. Jayasree Laha, and Prof. (Dr.) Ajit K. Mahapatra for their excellent teaching, unwavering support, and encouragement which have significantly enhanced the quality of my life. Also, sincere gratitude goes to Dr. Sudipta Chakraborty, Ranjit Das, and my elder brother Sankhasubra Maiti for their support through out my life.

I am also thankful to my esteemed colleagues and Pranab Kumar Barai, Head Master, Tatu Singha Smriti High School, Uttar Dinajpur for their valuable support and encouragement during my research work.

I express my thanks to the Department of Science and Technology-Fund for Improvement of Science and Technology Infrastructure (DST-FIST) for providing essential research infrastructure.

Finally, my deepest gratitude goes to the numerous individuals who have motivated, encouraged, and supported me in all my endeavors. Especially, I am indebted to my father, Rajkrishna Maiti whose unwavering support and encouragement have played a pivotal role in all my achievements. My sincere gratitude also goes to my beloved mother, brother, and aunts, Soma Maiti, Arpan Maiti, Rita Maiti, and Mita Maiti for their constant support throughout my life. Heartfelt thanks to my better half, Dr. Sudhir Kumar Das, for his constant encouragement during my research journey. Thanks to God for presenting me with the best gift in the world, my two little daughters, Brihasmita and Avigna whose love inspired me always to do better in my life. Last, but not least, I am highly grateful to the almighty for supporting me during my journey and encouraging me to perform best in my life.

Arpita Maiti

Research Scholar

Department of Chemistry
University of North Bengal
Darjeeling-734013, INDIA

List of Figures

Figures	Descriptions	Page No.
Figure 1.1:	Pictorial representations showing the various optical-based host-guest decorated systems.	3
Figure 1.2:	Pictorial presentation of the effect of binding of cation on the D- π -A system with spectral shifting in the absorption spectrum.	4
Figure 1.3:	Schematic representation of the photoinduced electron transfer (PET) process.	7
Figure 1.4:	Schematic illustration of ICT process.	8
Figure 1.5:	The photophysical cycle of the ESIPT process.	9
Figure-1.6:	Pictorial representations of AIE phenomena.	10
Figure 2.1:	Represent weighing balance used for the present thesis work	19
Figure 2.2:	Image of water distiller utilized for the present thesis work	20
Figure 2.3:	Demonstrate the image of the thermostat utilized for the present thesis work	20
Figure 2.4:	The image of the magnetic stirrer is used for the present thesis work.	20
Figure 2.5:	The image of the FT-IR spectrometer is used for the present thesis work	21
Figure 2.6:	The pictorial representation of the NMR spectrometer is used for the present thesis work.	22
Figure 2.7:	The image demonstrates the Agilent 6545XT Advance-Bio LC/Q-TOF spectrometer.	23
Figure 2.8:	The image represents the HITACHI U-2910 spectrophotometer.	23
Figure 2.9:	The pictorial representation of the benchtop spectrofluorimeter, HITACHI (F-7100).	24
Figure 3.1:	^1H NMR spectrum of our prepared probe DPAB in CDCl_3 .	28
Figure 3.2:	^{13}C NMR (CDCl_3 , 100 MHz) spectrum of DPAB in CDCl_3 .	28
Figure 3.3:	High-resolution mass spectra of our synthesized DPAB .	28
Figure 3.4:	The bar diagram demonstrates the change in absorption values of the DPAB-Al³⁺ complex at various percentages of water at 534 nm.	29

Figure 3.5:	(a) UV-visible absorption titration spectra of DPAB (5 μM) with different equivalents (0-28 equiv.) of Al^{3+} ions in DMSO. (b) Change in absorbance values of DPAB as a function of different Al^{3+} ions concentration in DMSO. (c) The corresponding ratiometric calibration plot.	31
Figure 3.6:	(a) UV-visible absorption titration spectra of DPAB (5 μM) with different equivalents (0-16 equiv.) of Al^{3+} ions in DMSO- H_2O (9:1 v/v) solution. (b) Change in absorbance of DPAB as a function of different Al^{3+} ions concentration in DMSO- H_2O (9:1 v/v) solution. (c) The corresponding ratiometric calibration plot.	31
Figure 3.7:	(a) Bar diagram demonstrating the change in absorbance values of DPAB with different divalent, trivalent cations and (b) various anions in DMSO- H_2O (9:1 v/v) medium at 534 nm. (c) Photograph of DPAB solution in the presence of 16 equiv. different metal ions.	32
Figure 3.8:	(a) Competition analysis of DPAB - Al^{3+} upon addition of different metal ions in DMSO- H_2O (9:1 v/v) medium. (b) Competition analysis of DPAB - Al^{3+} upon inclusion of different anions in DMSO- H_2O (9:1 v/v) medium.	33
Figure 3.9:	(a) UV-visible reversible absorption spectra of DPAB - Al^{3+} complex upon introducing PO_4^{3-} ions sequentially in DMSO- H_2O (9:1 v/v) medium. (b) Change of absorbance values of DPAB upon alternative inclusion of Al^{3+} and PO_4^{3-} ions subsequently in DMSO- H_2O (9:1 v/v) medium.	34
Figure 3.10:	UV-visible reversible absorption spectra of DPAB + Al^{3+} complex solution with the gradual addition of PO_4^{3-} DMSO.	34
Figure 3.11:	(a) Job's plot for the determination binding stoichiometric ratio of DPAB with Al^{3+} ions, (b) Benesi-Hildebrand plot to determine the interaction affinity of DPAB with Al^{3+} ions in DMSO- H_2O (9:1 v/v) medium.	36
Figure 3.12:	Left-Benesi-Hildebrand plot to determine the interaction affinity of DPAB with Al^{3+} ions in DMSO. Right- Job's plot	36

	for finding the stoichiometric interaction ratio of DPAB-Al³⁺ complex with PO₄³⁻ ions.	
Figure 3.13:	Left- Benesi-Hildebrand plot to determine the interaction affinity of Al³⁺ ions with PO₄³⁻ ions in DMSO. Right- Benesi-Hildebrand plot to determine the interaction affinity of Al³⁺ ions with PO₄³⁻ ions in DMSO-H ₂ O (9:1 v/v) medium.	37
Figure 3.14:	Left- The ratiometric calibration plot derived from changes in absorption values for finding out the detection limit in DMSO Right- DMSO-H ₂ O (9:1 v/v) medium.	38
Figure 3.15:	Colorimetric response time of DPAB and DPAB-Al³⁺ complex for the detection of (a) Al³⁺ and (b) PO₄³⁻ respectively.	39
Figure 3.16:	Estimation of the concentration of Al³⁺ added to various water samples following the standard curve.	39
Figure 3.17:	(a) Colorimetric change of DPAB -coated paper strips due to the inclusion of various metal ions. (b) Colorimetric change of DPAB -coated paper strips with the incorporation of different concentrations of Al³⁺ (10^{-4} M- 10^{-9} M). (c) Colorimetric change of paper strips-based test kit due to sequential Al³⁺ and PO₄³⁻ ions accumulations, respectively. (d) The visualization colorimetric change of the solid DPAB and (e) after adding drops of Al³⁺ (1 mM).	41
Figure 3.18:	(a) Visualization of bare eye colorimetric change of DPAB solution in introducing Al³⁺ ions. (b) The truth table for constructing YES molecular logic gate. (c) Representation of YES molecular logic circuit. (d) Visualization of bare eye colorimetric change of DPAB-Al³⁺ complex solution. (e) The corresponding truth table frames the NOT molecular logic gate. (f) Representation of NOT molecular logic circuit.	42
Figure 3.19:	(a) Colorimetric change of DPAB solution upon successive addition of Al³⁺ and PO₄³⁻ ions in DMSO-H ₂ O (9:1 v/v) medium (b) Bar diagram representing the change in absorbance at 534 nm as optical outputs. (c) The truth table	43

	for constructing the INHIBIT molecular logic gate. (d) Representation of INHIBIT logic circuit.	
Figure 3.20:	(a) The subsequent logic circuit of the memory device and (b) its truth table (c) Reversible logic operations with "Writing-Reading-Erasing-Reading" behavior are displayed by the feedback loop.	44
Figure 3.21:	(a) The RGB color responses of our DPAB probe for quantifying the Al ³⁺ ions. (b) Calibration curve of Al ³⁺ ions vs R/G to estimate the LOD value with the help of a smartphone-based readout technique.	45
Figure 4.1:	¹ H NMR spectrum (CDCl ₃ , 400 MHz) of BPH .	57
Figure 4.2:	¹³ C NMR spectrum (CDCl ₃ , 100 MHz) of BPH .	58
Figure 4.3:	(a) UV-visible absorption titration spectra of our probe BPH due to the stepwise addition of DCP in ACN solvent. (b) Image of BPH -solution of the phosphorylated and non-phosphorated one. Photos are taken in normal light with 6 mM DCP additions. (c) Linear calibration plot log(A ₅₂₀ /A ₄₂₀) vs. [DCP] (M) to understand the absorbance spectral change during titration.	59
Figure 4.4:	UV-visible titration spectra of BPH with the excess additions of DCP.	59
Figure 4.5:	(a) Change in photoluminescence spectra of BPH with gradual additions of DCP in ACN solvent at λ _{ex} = 380 nm. (Inset: demonstration of the colorimetric change in photoluminosity due to the addition of DCP in BPH solution) (b) Change in photoluminescence intensity of BPH with incremental additions of DCP in ACN solvent. (c) Color chromatography diagram of probe BPH and DCP phosphorylated BPH + DCP in ACN solvent with co-ordinate values have been shifted from x = 0.159, y = 0.073 to x = 0.166, y = 0.299 respectively at λ _{ex} = 380 nm.	60
Figure 4.6:	Change in photoluminescence spectra of BPH with gradual additions of DCP in ACN solvent at λ _{ex} = 350 nm.	61

Figure 4.7:	(a) Bar diagrams demonstrate the changes of photoluminescence intensity of BPH solution at 503 nm with additions of DCP and other OPs and IPs to find its selectivity. (b) Colorimetric change of BPH solution in the presence of sarin stimulant DCP and other toxic analytes in daylight. (c) Change of photoluminescence of BPH solution in the presence of sarin stimulant DCP and other toxic analytes under a 365 nm UV lamp.	62-63
Figure 4.8:	Linear calibration curve between fluorescence intensity vs. concentration of DCP at 503 nm to estimate LOD and LOQ values towards sensing of DCP employing BPH.	64
Figure 4.9:	(a) Visual colorimetric change of BPH fabricated paper strips under daylight in the presence of DCP and other analytes. Representative photograph on BPH-dipped paper strips upon exposure to various concentrations of DCP, including 10^{-6} , 10^{-5} , 10^{-4} , 10^{-3} , 10^{-2} , and 10^{-1} M under (b) daylight (d) a 365 nm UV lamp irradiation. (c) Image displaying a fluorimetric change of BPH fabricated paper strips under a 365 nm UV irradiation in the presence of DCP and other analytes.	65
Figure 4.10:	(a) Pictorial representation of BPH-loaded filter paper upon displaying fluorescence response due to the exposure of sarin gas mimic vapor with various analogous analytes under a 365 nm UV lamp. (b) Investigating the dip-stick method at different DCP concentrations, such as 10^{-6} , 10^{-5} , 10^{-4} , 10^{-3} , 10^{-2} , and 10^{-1} M, for quantitative detection of sarin substitute DCP. Photograph of the color (c) and fluorescence (d) of probe BPH before and after the exposure of DCP vapor, conducted in the conical flask.	66
Figure 5.1:	^1H NMR spectrum of HDBQ in CDCl_3 .	75
Figure 5.2:	^{13}C NMR spectrum of HDBQ in CDCl_3 .	76
Figure 5.3:	FT-IR spectrum of HDBQ.	76
Figure 5.4	High-resolution mass spectra of HDBQ.	76
Figure 5.5:	Normalized UV-visible absorption and emission spectra of	77

	HDBQ in DMSO solvent.	
Figure 5.6:	(a) UV-visible absorption spectra of probe- HDBQ (1.2×10^{-5} M) in a 20% (v/v) water-DMSO reaction mixture due to the presence of various concentrations of Cu^{2+} ions (b) Change in absorbance intensity values with a gradual increment of Cu^{2+} ions concentration at 492 nm.	78
Figure 5.7:	(a) Emission titration spectra of HDBQ (1.2×10^{-5} M) in a 20% (v/v) water-DMSO due to the stepwise inclusion of Cu^{2+} ions (b) Change in fluorescence intensity with the gradual addition of Cu^{2+} ions at 514 nm.	79
Figure 5.8:	Representation of (a) UV-visible spectrophotometric and (b) fluorescence metal selectivity bar diagram feeding absorbance values and emission intensity at 492nm and 514 nm, respectively. Representation of (c) UV-visible spectrophotometric metal ions interference bar diagram displaying absorbance values at 492 nm and (d) Fluorescence anion interference bar diagram showing emission intensity at 514 nm. Pictorial representation HDBQ solution in a 20% (v/v) water-DMSO in the inclusion of different metal ions (e) under normal light and (f) under a handy 365 UV lamp.	80-81
Figure 5.9:	Anion selectivity bar diagram displaying change in absorbance values at 492 nm in the UV-visible absorption spectra. (b) The anion selectivity bar diagram shows the change in fluorescence intensity at 514 nm.	81
Figure 5.10:	Anion interference bar diagram showing the change in absorbance values at 492 nm in the UV-visible absorption spectra.	82
Figure 5.11:	The calibration curve to estimate LOD and LOQ values of Cu^{2+} ions was determined by feeding the fluorescence intensity of HDBQ at 514 nm in a 20% (v/v) water-DMSO under ambient conditions.11	82
Figure 5.12:	Fluorescence response time study of HDBQ towards Cu^{2+} ions showing fluorescence intensity at 514nm in a 20%(v/v) water-	84

	DMSO mixture.	
Figure 5.13:	pH metric analysis fluorescence intensity change at 510 nm.	84
Figure 5.14:	FT-IR spectra of HDBQ and Cu^{2+} ions chelated HDBQ complex.	85
Figure 5.15:	Partial ^1H NMR titration spectra of HDBQ in the presence of Cu^{2+} ions.	86
Figure 5.16:	High-resolution mass spectra of Cu^{2+} ions chelated HDBQ complex.	86
Figure 5.17:	(a) Normalized Job's plot to find the stoichiometric ratio in the HDBQ-Cu²⁺ ions complex feeding emission intensity at 514 nm. The plot represents the Stern-Volmer analysis for the determination of the (b) static quenching and (c) dynamic quenching constant due to the formation of Cu^{2+} ions of the HDBQ chelate complex.	87
Figure 5.18:	Binding stability isotherm of Cu^{2+} ions with HDBQ from fluorescence titration curve.	88
Figure 5.19:	Reversibility (a) UV-visible spectrometric and (b) fluorescence titration spectra of HDBQ-Cu²⁺ ions complex due to the addition of EDTA in a 20% (v/v) water-DMSO solution. (c) The change of fluorescence intensity of HDBQ solution at 514 nm due to the successive addition of Cu^{2+} ions and EDTA.	89
Figure 5.20:	Operation of the INHIBIT logic gate: (a) The bar diagram represents the fluorescence intensity as optical output. (b) The fluorometric color change was observed under 365nm UV light due to the introduction of Cu^{2+} ions and EDETA as optical outputs. (c) Formation of the truth table for the formation of the INHIBIT logic gate. (d) Pictorial representation of INHIBIT logic circuit.	90
Figure 5.21:	(a) Colorimetric change of HDBQ -coated paper strip-based test kit in the presence of various metal ions in daylight. (b) The fluorimetric change of HDBQ -dopped paper in addition to different metal ions under handy 365 UV lamp irradiation.	91
Figure 6.1:	^1H NMR spectra BDPA in CDCl_3 .	100

Figure 6.2:	^{13}C NMR spectra BDPA in CDCl_3 .	100
Figure 6.3:	High-resolution mass spectra of BDPA with $m/z = 423.2547$	101
Figure 6.4:	(a) UV-visible spectrophotometric titration spectra of BDPA (5.6 μM) due to gradual addition, 0- 33 equiv., of DCP in pure ACN medium and (b) change of absorbance values at 418 nm and 554 nm with increasing concentration of DCP. [Inset: Demonstrate the ratiometric linear calibration curve [DCP] vs. $\log (A_{554}/A_{418})$.] (c) The linear calibration curve [DCP] vs. absorbance values for determination of limit of detection. (d) Change in absorbance values in the attendance of 33 equiv. sarin substitute DCP and other competitive toxic analogous analytes. (e) Snapshot on colorimetric change of BDPA solution in the attendance of sarin surrogate DCP and other harmful competing analytes.	103
Figure 6.5:	(a) Absorption titration spectrum of BDPA (5.9 μM) due to steady addition, 0- 17 equiv., of DCP in acetonitrile-water (9:1) medium and (b) change of absorbance intensity values at 426 nm and at 540 nm with increasing concentration of DCP. [Inset: The ratiometric [DCP] Vs. $\log (A_{540}/A_{426})$ linear calibration curve.]	103
Figure 6.6:	Change of UV-visible absorbance intensity of BDPA -DCP at different percentages of water.	107
Figure 6.7:	(a) Change in absorbance values in the attendance of 33 equiv. sarin substitute DCP and other competitive toxic analogous analytes. (b) Snapshot on colorimetric change of BDPA solution in the attendance of sarin surrogate DCP and other harmful competing analytes.	105
Figure 6.8:	(a) The UV-visible absorption reversible titration spectrum of BDPA upon gradually adding TEA (0 – 1) equiv. in pure ACN. (b) Changes in the absorption maximum of the BDPA solution with alternating DCP and ammonia vapor exposure. (c) Plausible reaction mechanism of BDPA with DCP and its rebirthing after introducing TEA.	116

Figure 6.9:	The UV-visible absorption reversible titration spectrum of BDPA-DCP upon steady addition of 1 equiv. TEA in acetonitrile-water (9:1) solvent.	107
Figure 6.10:	Job's plot for the binding of BDPA with DCP.	108
Figure 6.11:	High-resolution mass spectra of BDPA-DCP adduct with $m/z = 767.28$.	109
Figure 6.12:	^1H NMR titration of BDPA with DCP and TEA sequentially.	109
Figure 6.13:	(a) Selectivity experiment demonstration by utilizing fabricated BDPA -loaded paper strips in the attendance of various analogous poisonous guest analytes. (b) Typical image of paper strips coated with BDPA after exposure to different DCP concentrations. (c) Demonstration of the transportable paper strips-based handmade test kit utilizing consecutive detection of DCP and TEA by color changing blue to light red five times.	110
Figure 6.14:	(a) Demonstration of the dipstick experiment of our developed chromogenic probe BDPA in the attendance of various analogous toxic analytes vapor. (b) Dipstick experiment at various concentrations, including 10^{-9} , 10^{-8} , 10^{-7} , 10^{-6} , 10^{-5} , 10^{-4} , and 10^{-3} M for the quantification of sarin surrogate DCP. (c) Images of the colorimetric change chromogenic probes (i) before and (ii) after capturing DCP gas, taken in the conical flask. (d) Time-dependent absorbance values change of BDPA and BDPA-DCP adduct at 612 nm over (0-6) min. period. (e) Dipstick experiment study 0-6 min. time duration. (f) The BDPA solution's color change concerning time, demonstration via sealed vial experiment.	112-113
Figure 6.15:	The response of the DCP gas detection under different humidity conditions.	113
Figure 6.16:	(a) The BDPA probe's RGB color responses to quantify DCP. (b) The calibration curve generated by B/G vs. [DCP] utilizing a smartphone-based readout method to estimate the LOD value.	115
Figure 7.1:	^1H NMR spectra of our synthesized BD1 .	126

Figure 7.2:	^{13}C NMR spectra of our synthesized BD1 .	126
Figure 7.3:	DEPT-90 NMR spectra of our synthesized BD1 .	127
Figure 7.4:	DEPT-135 NMR spectra of our synthesized BD1 .	127
Figure 7.5:	COSY NMR spectra of our synthesized BD1 .	128
Figure 7.6:	HMQC NMR spectra of our synthesized BD1	128
Figure 7.7:	FT-IR Spectra of our synthesized BD1 .	129
Figure 7.8:	High-resolution mass spectra (HRMS) of our synthesized BD1 .	129
Figure 7.9:	(a) UV-visible absorption titration spectra of BD1 with the gradual addition of Zn^{2+} ions, (b) absorbance values change at 370 nm & 430 nm due to the accumulation of Zn^{2+} ions. (c) Linear calibration curve $\log (A_{370\text{nm}}/A_{430\text{nm}})$ vs. $[\text{Zn}^{2+}]$ to estimate the unknown concentration of Zn^{2+} ions with minimal experimental error.	131
Figure 7.10:	(a) The photoluminescence titration spectra of BD1 due to the gradual addition of Zn^{2+} ions, (b) corresponding CIE diagram of BD1 and Zn^{2+} chelated BD1 complex.	132
Figure 7.11:	(a) Visual colorimetric changes of BD1 solution under the exposure of a 365 nm UV due to the addition of various metal ions a= BD1 , b= Zn^{2+} , c= Al^{3+} , d= Ba^{2+} , e= Ca^{2+} , f= Cd^{2+} , g= Co^{2+} , h= Cr^{3+} , i= Cu^{2+} , j= Fe^{2+} , k= Fe^{3+} , l= Hg^{2+} , m= Mg^{2+} , n= Mn^{2+} , o= Ni^{2+} , p= Pb^{2+} . (b) The bar diagrams display the selectivity of our BD1 towards various Zn^{2+} ions.	133
Figure 7.12:	The emission intensity change of the Zn^{2+} - BD1 complex is due to the accumulation of various anions.	134
Figure 7.13:	(a) Job's plot for finding the stoichiometric ratio between BD1 and Zn^{2+} ions in the Zn^{2+} chelated BD1 complex. (b) Linear calibration curve for finding the LOD and LOQ values, (c) The linear graph for finding the apparent stability constant of the Zn^{2+} ions chelated BD1 complex.	135
Figure 7.14:	FT-IR spectra of BD1 and Zn^{2+} ions chelated BD1 complex.	136
Figure 7.15:	^1H NMR spectra of BD1 and BD1 chelated Zn^{2+} complex.	136
Figure 7.16:	(a) Photoluminescence titrations spectrum of Zn^{2+} ions	137

	chelated BD1 complex solution upon gradual introduction of HSO_4^- ions (0.0–0.62 mM) in DMF, (b) The linear fitting plot of fluorescence intensity vs. $[\text{HSO}_4^-]$ for calculation of detection limit.	
Figure 7.17:	(a) Photoluminescence titration spectra of Zn^{2+} - BD1 chelated complex due to the gradual introduction of PA. (b) The bar diagram displays the selectiveness of the Zn^{2+} ions chelated BD1 complex towards the recognition of the PA system among the numerous NACs, showing photoluminescence intensity at 475 nm obtained from the Zn^{2+} ions chelated BD1 complex.	139
Figure 7.18:	The plot of $\left[\frac{I_0}{I} - 1\right] \frac{1}{[\text{PA}]}$ against $[\text{PA}]$ for finding out the dynamic quenching constant from the photoluminescence titration of the BD1 chelated Zn^{2+} complex.	139
Figure 7.19:	The plot of the fluorescence intensity of BD1 chelated Zn^{2+} complex against $[\text{PA}]$ to find out the detection limit.	140
Figure 7.20:	Fluorescence intensity changes of the BD1 chelated Zn^{2+} complex in addition to PA in the presence of other competing NACs.	140
Figure 7.21:	(a) Truth table of the constructed INHIBIT logic circuit, (b) corresponding pictographic presentation of the logic circuit, (c) bar diagram displaying the fluorescence intensity observed at 475 nm, (d) pictorial presentation of color changes of the BD1 solution under 365 UV light irradiation.	141
Figure 7.22:	(a) The fluorogenic colorimetric observation of the BD1 -loaded test kit after the introduction of different metal ions under the exposure of a 365 nm UV lamp. (b) The fluorogenic colorimetric change of the BD1 loaded test kit due to the sequential addition of Zn^{2+} and PA under a 365 nm UV light treatment.	142

List of Tables

Tables	Descriptions	Page No.
Table 3.1:	Determination of Al ³⁺ ions in the water sample.	39
Table 3.2:	Comparison with the detection limits of sensing Al ³⁺ ions by various sensors.	46
Table 3.3:	Comparison with the detection limits of sensing PO ₄ ³⁻ ions by various sensors.	48
Table 4.1:	Comparison table of different chemosensors that have been introduced for the detection of DCP in the last few decades with our prepared BPH .	67
Table 5.1:	UV-visible absorption and fluorescence spectral parameters of probe HDBQ with varying the polarity of the solvents medium (nm)	78
Table 5.2:	Comparison of various methods and chemosensors towards the detection of Cu ²⁺ ions.	83
Table 5.3:	Detection of Cu ²⁺ ions in various practical water samples	92
Table 6.1:	Toxicological data of key chemical warfare agents.	111
Table 6.2:	Comparison table of various chemosensors introduced to detect DCP in the last few decades with our BDPA .	115
Table 7.1:	Comparison of different Zn ²⁺ ions chemosensor and their specifications.	142

List of Schemes

Schemes	Descriptions	Page No.
Scheme 3.1:	Synthetic scheme of cinnamaldehyde-derived chemosensor (DPAB).	27
Scheme 3.2:	The probable colorimetric sensing mechanism for sequential recognition of Al ³⁺ and PO ₄ ³⁻ ions.	35
Scheme 4.1:	Structure of nerve agents and their mimics.	54
Scheme 4.2:	Synthetic route for the preparation of BPH.	57
Scheme 5.1:	Synthetic route for the preparation of HDBQ.	75
Scheme 5.2:	Complexation route between HDBQ and Cu ²⁺ ions.	85
Scheme 5.3:	Formation Cu ²⁺ ions chelated HDBQ complex and its reversibility by EDTA.	89
Scheme 6.1:	General chemical structures of nerve agents and their potential mimics.	97
Scheme 6.2:	Synthetic pathway for preparing our probe BDPA.	100
Scheme 7.1:	The mechanistic pathway for the preparation of BD1.	126
Scheme 7.2:	The mechanistic aspects for the successive detection of Zn ²⁺ and HSO ₄ ⁻ ions.	138

List of Appendices

Appendix	Page No.
I. List of Publications	169
II. List of Seminars/Conferences/Workshops Attended	170